Communication

AFM Study of the Influence of Stopped Glycerol Flow in a Coil on Peroxidase Enzyme

Yuri D. Ivanov *, Ivan D. Shumov, Andrey F. Kozlov, Anastasia A. Valueva, Maria O. Ershova, Irina A. Ivanova, Alexander N. Ableev, Vadim Y. Tatur, Andrei A. Lukyanitsa, Nina D. Ivanova, Vadim S. Ziborov

Posted Date: 6 March 2024

doi: 10.20944/preprints202403.0304.v1

Keywords: horseradish peroxidase; glycerol; atomic force microscopy; enzyme aggregation

Communication

AFM Study of the Influence of Stopped Glycerol Flow in a Coil on Peroxidase Enzyme

Yuri D. Ivanov [1,2,*], Ivan D. Shumov [1], Andrey F. Kozlov [1], Anastasia A. Valueva [1], Maria O. Ershova [1], Irina A. Ivanova [1], Alexander N. Ableev [1], Vadim Y. Tatur [3], Andrei A. Lukyanitsa [3,4], Nina D. Ivanova [3,5] and Vadim S. Ziborov [1,2]

[1] Institute of Biomedical Chemistry, Pogodinskaya Str., 10 Build. 8, Moscow 119121, Russia; shum230988@mail.ru (I.D.S.); afkozlow@mail.ru (A.F.K.); varuevavarueva@gmail.com (A.A.V.); motya00121997@mail.ru (M.O.E.); i.a.ivanova@bk.ru (I.A.I.); ableev@mail.ru (A.N.A); ziborov.vs@yandex.ru (V.S.Z.)
[2] Joint Institute for High Temperatures of the Russian Academy of Sciences, Moscow 125412, Russia
[3] Foundation of Perspective Technologies and Novations, Moscow 115682, Russia; v_tatur@mail.ru (V.Y.T.); andrei_luk@mail.ru (A.A.L.); ninaivan1972@gmail.com (N.D.I.)
[4] Moscow State University, Faculty of Computational Mathematics and Cybernetics, 119991 Moscow, Russia
[5] Moscow State Academy of Veterinary Medicine and Biotechnology Named after Skryabin, Moscow 109472, Russia
* Correspondence: yurii.ivanov.nata@gmail.com

Abstract: Glycerol represents a useful functional component of heat-transfer fluids. Glycerol is known to be triboelectrically active. We report how the flow of glycerol, stopped in a cylindrical coiled pipe, influences horseradish peroxidase (HRP) enzyme. Namely, glycerol flow was pumped through the coil and then stopped. After that, we incubated the 0.1 μM solution of HRP near the side of the coil, and then adsorbed HRP onto mica. This operation markedly increased the HRP aggregation on mica in comparison with the control sample. We explain this phenomenon by the influence of triboelectrically induced electromagnetic fields. Our results can be useful in the development of flow-based systems for biosensors and bioreactors.

Keywords: horseradish peroxidase; glycerol; atomic force microscopy; enzyme aggregation

1. Introduction

Enzymes have found numerous applications in biotechnology [1] and biomedical science [2]. In nature, enzymes catalyze reactions in living cells [3], and can be employed as catalysts in a wide range of commercially important processes [1]. The list of biotechnological applications of enzymes includes, for instance, food processing, synthesis of pharmaceuticals, paper fabrication, etc. [1,4]. In biomedical science, applications of enzymes in biosensors [2] and in diagnostic test kits [5,6] should be mentioned.

Enzyme-based catalysis requires proper selection and careful maintaining of optimal process conditions, since enzymes quickly lose their functional activity at extreme temperatures [7], pH values, ion concentrations, and pressures [8]. This is why biosensors and bioreactors intended for operation with enzymes are often equipped with thermal stabilization systems in order to maintain stable temperature conditions [9,10]. In these thermal stabilization systems, cylindrically wound pipes (or simply coils) with circulating heat-transfer fluid are often employed [11–13]. The use of glycerol as a component of heat-transfer fluids was shown to be promising [14,15]. At that, it should be emphasized that the flow of glycerol in a pipe induces electromagnetic fields due to the so-called triboelectric effect [16,17]. Electromagnetic fields generated upon flow of glycerol can be quite strong [16], thus representing an important factor influencing the activity of enzymes [18]. The effect of a

 doi:10.20944/preprints202403.0304.v1

triboelectrically induced field on an enzyme can take place even after stopping the flow of heat transfer fluid [18].

One of possible effects of electromagnetic fields on an enzyme is exhibited in a form of a change in its aggregation state on upon adsorption onto a solid substrate surface [18–20]. This is an important point, since surface-adsorbed enzymes are widely employed in biotechnology [1]. Aggregation of proteins, including enzyme proteins, is generally attributed to misfolding or partial unfolding of their polypeptide chains [21,22]. With regard to enzymes, their aggregation can also be related to a change in their hydration [18,19,23–25]. In general, aggregation is considered to cause a decrease in the functional activity of enzymes [26]. Colombie' et al. demonstrated that inactivation of lysozyme in a bioreactor is accompanied by its aggregation [27]. On the other hand, Gentile et al. emphasized that aggregation of an enzyme can occur in the course of its functioning and does not inevitably imply the activity loss [28]. Accordingly, enzyme aggregation and external factors, influencing this process, require further thorough investigation. In this respect, ultrasensitive methods such as atomic force microscopy (AFM) are of use [18,19,29–31], since they allow the researchers to reveal even subtle effects on the enzyme aggregation [31].

Horseradish peroxidase (HRP) is a ~44 kDa enzyme glycoprotein [32,33]. It is widely employed in diagnostic kits as a component of enzyme-linked immunosorbent assay (ELISA) kits [34], and in biosensors as a reporter enzyme [35]. Furthermore, HRP has found many industrial applications in food technology [36], wastewater purification [37] and biofuel cells [38–40]. At that, aggregation state of HRP was shown to be influenced by external magnetic [29,30] and electromagnetic fields [18–20]. Electromagnetic fields are ubiquitous in industry [41]. As mentioned above, the aggregation state of enzymes can influence their functional activity. This explains the importance of further in-deep investigation of the influence of electromagnetic fields on the aggregation state of HRP.

Our present study reveals a considerable 40-minute aftereffect (the so-called long-term effect [19]) of the glycerol flow in a cylindrically coiled heat exchanger on the aggregation state of HRP after incubation of its solution near the outer side of the coiled section. In other words, the glycerol flow has been stopped prior to the incubation of the enzyme. The enzymatic activity of HRP has been found unaffected — as opposed to the previously reported case with the incubation of the enzyme near the inlet section of the heat exchanger [19]. Nevertheless, a considerably increased content of aggregated enzyme has been revealed by AFM on the surface of mica substrates after the incubation of the enzyme in our experimental setup. The phenomenon observed can be explained by the influence of triboelectrically induced electromagnetic fields [20].

2. Materials and Methods

2.1. Chemicals and Protein

Glycerol was purchased from Glaconchemie GmbH (Merseburg, Germany). Both the HRP enzyme (peroxidase from horseradish; cat. #6782) and its substrate 2,2′-azino-bis(3-ethylbenzothiazoline-6-sulfonate) (ABTS; cat. #A-1188) were purchased from Sigma (St. Louis, MO, USA). Disodium hydrogen orthophosphate, citric acid and hydrogen peroxide (H_2O_2) were purchased from Reakhim (Moscow, Russia). 2 mM Dulbecco's modified phosphate buffered saline (PBSD buffer) was prepared by dissolving the salt mixture purchased from Pierce (USA) in appropriate amount of ultrapure water. In all experiments, deionized ultrapure water (with 18.2 MΩ × cm resistivity), obtained with a Simplicity UV system (Millipore, Molsheim, France), was used.

The enzyme samples tested in the experiments represented 0.1 μM HRP solutions in 2 mM PBSD.

2.2. Experimental Setup and Enzyme Treatment

In general, the experimental setup was similar to that used in our previous study [19], but the enzyme was incubated near the heat exchanger's coiled section. The location of the tested HRP solution (working sample) is schematically shown in Figure 1.

 doi:10.20944/preprints202403.0304.v1

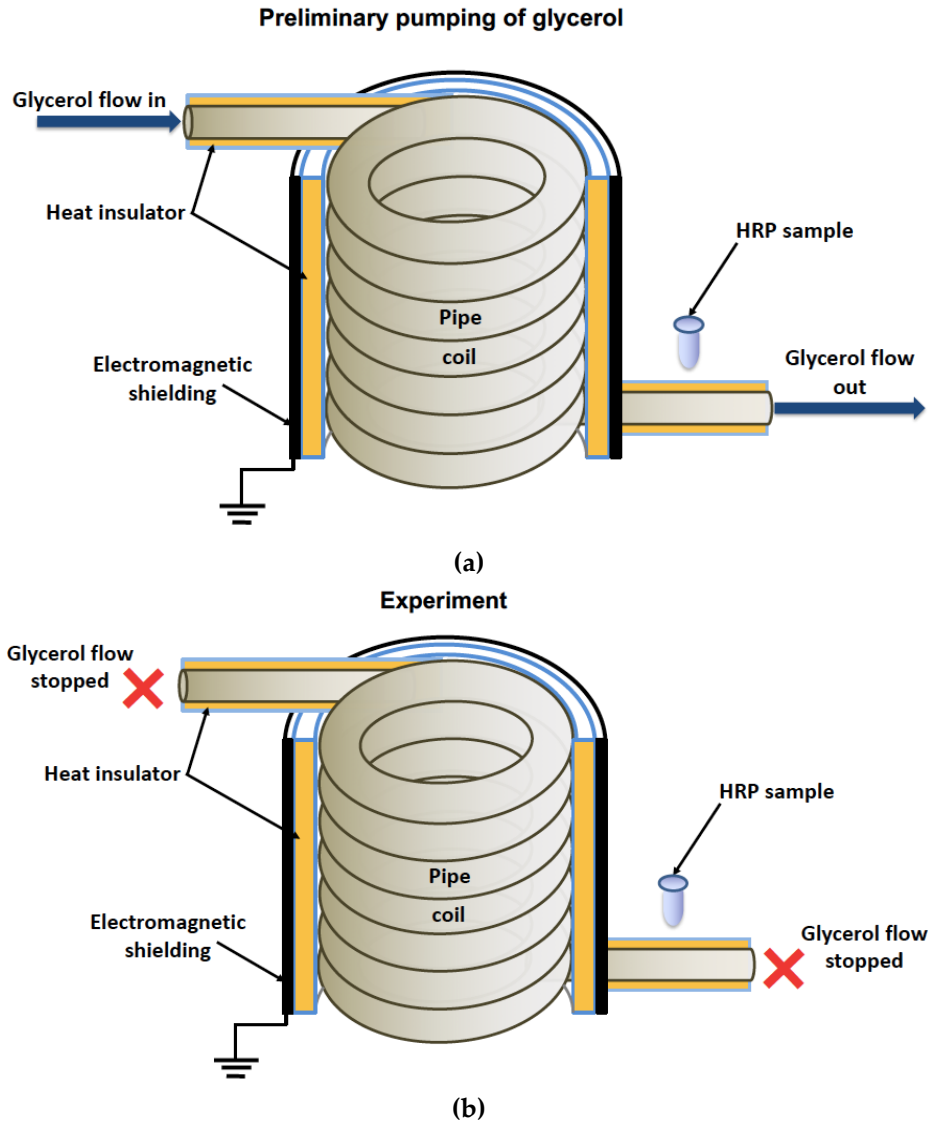

Figure 1. Schematic of the experimental setup illustrating the preliminary pumping of glycerol (a) and the incubation of the enzyme solution (working sample) near the coiled section of the heat exchanger after stopping the glycerol flow (b).

The cylindrically wound polymeric pipe modeled the heat exchanger. Prior to the experiment, warm glycerol had been continuously pumped through the heat exchanger at a flow rate of 9 L/s and a temperature of 65°C for 40 min. The use of warm glycerol was required to provide enough fluidity and, hence, the desired flow rate.

After the 40-min-long pumping, the glycerol flow was stopped, and working sample of the enzyme solution (1 mL in a 1.7-mL polypropylene single-use Eppendorf-type test tube) was incubated near (at a 2 cm distance) the heat-insulating cover of the heat exchanger for 40 min. The heat insulating cover allowed us to avoid undesired heating of the enzyme sample (which can affect its activity [36]), so that the enzyme incubation was performed at room temperature. Control sample of the enzyme (1 mL in a 1.7-mL polypropylene single-use Eppendorf-type test tube) was placed three meters away from the experimental setup. Both the working and the control enzyme samples were then subjected to AFM and spectrophotometry analysis.

2.3. Preparation of Substrates and Atomic Force Microscopy Measurements

Enzyme from both the working and the control samples was directly adsorbed onto 7 mm×15 mm pieces of freshly cleaved mica, which were used as AFM substrates, as described in our previous

 doi:10.20944/preprints202403.0304.v1

papers [18–20] according to Kiselyova et al. [42]. Briefly, the substrate was immersed into the 1.7-mL Eppendorf-type tube, which contained 0.8 mL of the respective enzyme sample, and incubated therein for ten minutes at room temperature and 600 rpm. After this incubation, the substrate was washed with deionized water and dried in air. Each of the so-prepared substrates was then placed into a Titanium atomic force microscope (NT-MDT, Zelenograd, Russia), which was equipped with NSG10 cantilevers (TipsNano, Zelenograd, Russia; resonant frequency 47–150 kHz, force constant from 0.35 to 6.1 N/m). The AFM scanning was carried out in a semi-contact mode in air at a temperature of 25°C. The size of each scan was either 1×1 μm^2 or 2×2 μm^2, and the scanning resolution was 256×256. For each substrate, at least 16 scans in different areas of the substrate were obtained.

For each AFM substrate (that is, for each enzyme sample studied), we calculated the total number of objects visualized in the AFM images, which was no less than 200. The distributions of the relative number of objects with height $\rho(h)$ (density functions) were calculated for each sample studied, as was described previously by Pleshakova et al. [43]:

$$\rho(h)=(N_h/N)\times 100\%, \quad (1)$$

where N_h is the number of objects with height h, and N is the total number of the visualized objects. In blank experiments, which were performed with protein-free buffer instead of enzyme solution in order to estimate the number of non-specifically adsorbed objects on the substrate surface, no objects with heights exceeding 0.5 nm was registered.

For each sample studied, absolute number of AFM-visualized particles, normalized per 400 μm^2, was also calculated according to Pleshakova et al. [43]:

$$N_{400}=400\times N/A, \quad (2)$$

where A is the total area of all AFM scans obtained for each sample.

Atomic force microscope operation and further processing of AFM images (alignment, flattening correction, export to ASCII format, etc.) were performed using the standard NOVA Px software (NT-MDT, Moscow, Zelenograd, Russia) supplied with the microscope. The number of the visualized particles in the obtained AFM images was calculated automatically using a specialized AFM data processing software, which was developed in the Institute of Biomedical Chemistry.

2.4. Spectrophotometry Analysis

The spectrophotometry measurements were performed in order to estimate whether there is a change in enzymatic activity of HRP against ABTS in the sample incubated near the coil with stopped flow of glycerol. We employed the technique developed by Sanders et al. [44], performing the measurements at 405 nm in phosphate-citrate buffer [44,45] (pH 5.0) in 1 cm quartz spectrophotometric cell for 5 minutes. The solution in the cell contained 1 nM HRP, 0.3 mM ABTS and 2.5 mM hydrogen peroxide.

3. Results

In our experiments, the working enzyme sample was incubated near the coiled heat exchanger with stopped flow of glycerol — namely, at a 2 cm distance from the outer side of the coil. At the same time, the control enzyme sample was kept three meters away from the experimental setup. Figure 2 displays typical AFM images of HRP particles adsorbed onto mica substrates after the incubation in either the working or the control enzyme sample.

 doi:10.20944/preprints202403.0304.v1

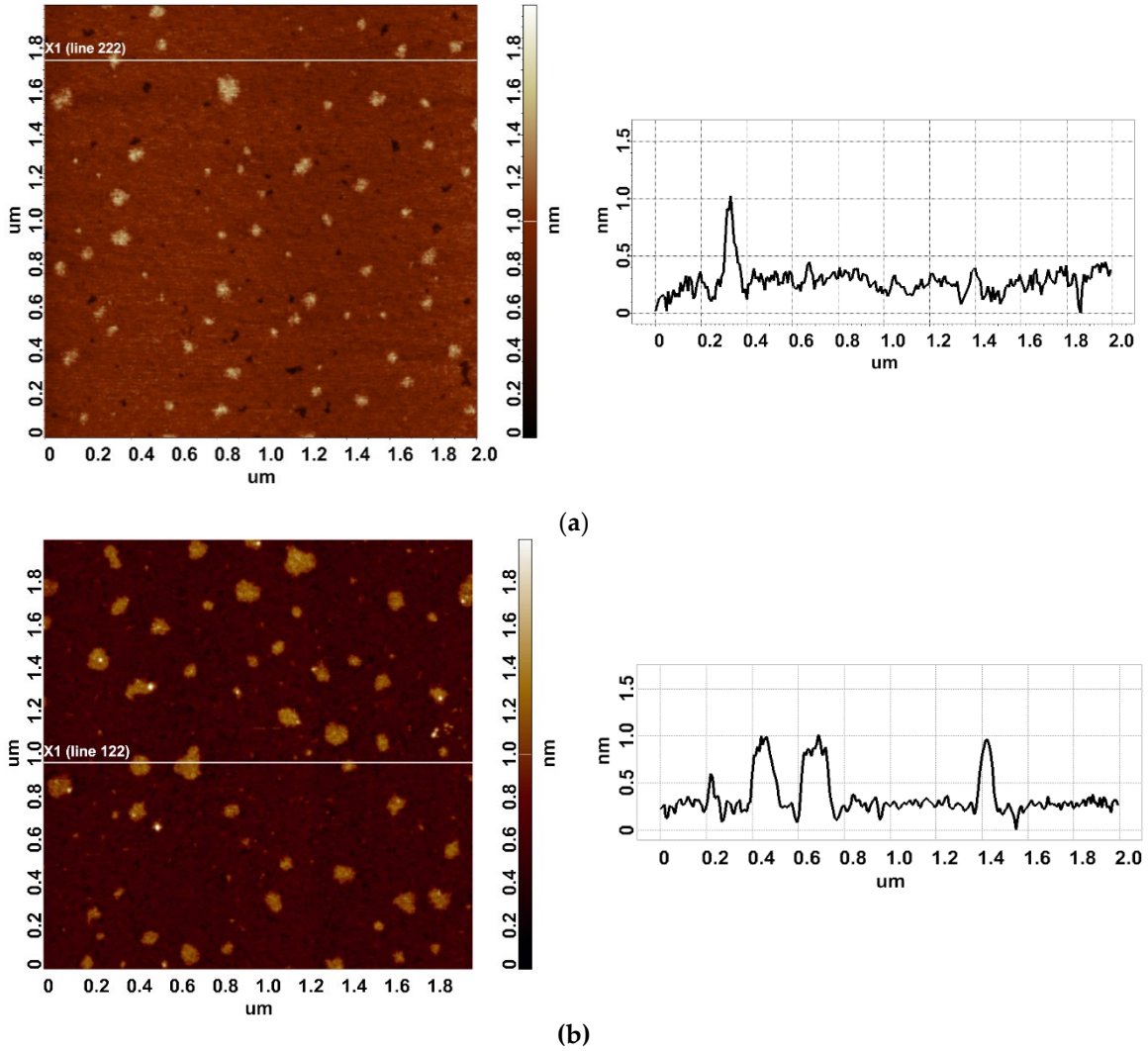

Figure 2. Typical AFM images of HRP particles adsorbed on mica from the control (**a**) and the working (**b**) enzyme samples. Right panels display the cross-section profiles corresponding to the lines in the AFM images shown in the respective left panels.

In the both AFM images shown in Figure 2 one can see compact objects of 1 to 1.2 nm height, which corresponds to the height of mica-adsorbed HRP [20]. In blank experiments, no objects of>0.5 nm height was visualized. In order to find out whether there is any difference between the HRP adsorption from the working sample and the control one, the density function ($\rho(h)$) plots obtained for these samples have been analyzed. These $\rho(h)$ plots are shown in Figure 3.

 doi:10.20944/preprints202403.0304.v1

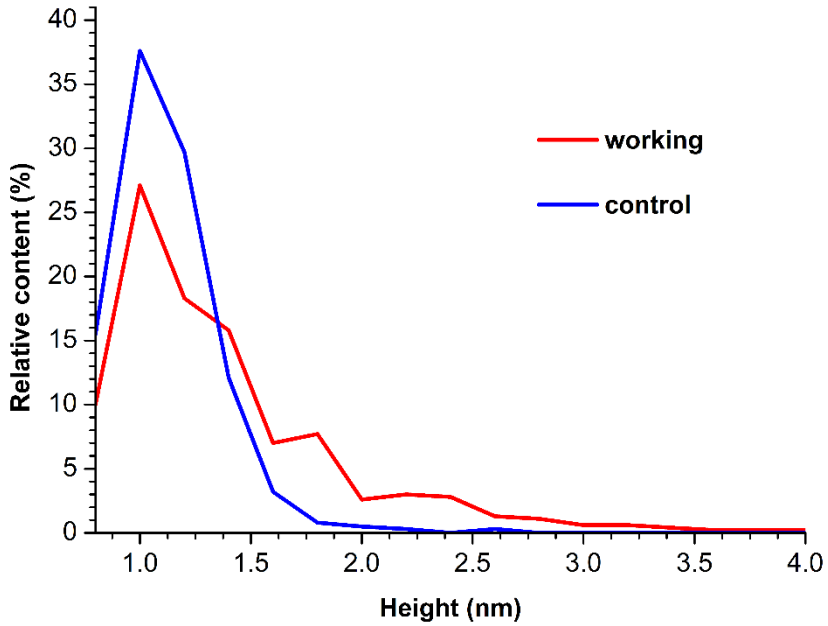

Figure 3. Density function plots obtained for control (black curve) and working (red curve) HRP samples.

The curves shown in Figure 3 indicate that for the control enzyme sample, the maximum of the respective density function corresponds to $h_{max}(control)$ = 1.0 ± 0.2 nm, while its width at half-height (WHH [43]) makes up $WHH(control)$ = 0.5 nm. As was mentioned above, the height of AFM images of monomeric HRP is 1.0 to 1.2 nm. Based on this, objects of this height, observed on the mica surface, can be attributed to HRP monomers.

For the working enzyme sample, the maximum of the respective density function was similar to that observed for the control one: $h_{max}(working)$ = 1.0 ± 0.2 nm. At that, the distribution obtained for the working sample was considerably broader: $WHH(working)$ = 0.7 nm. The broader $\rho(h)$ sample indicates an increased aggregation of HRP in the working sample in comparison with the control one, since the objects of greater heights can well be attributed to aggregated enzyme [20]. Furthermore, an increased contribution of particles with heights >1.4 nm was observed in comparison to the control sample, and this is the second fact indicating increased aggregation of HRP.

Figure 4 displays histograms of absolute number of AFM-visualized particles, normalized per 400 μm² (N_{400}), plotted vs. height.

Preprints.org (www.preprints.org) | NOT PEER-REVIEWED | Posted: 6 March 2024 doi:10.20944/preprints202403.0304.v1

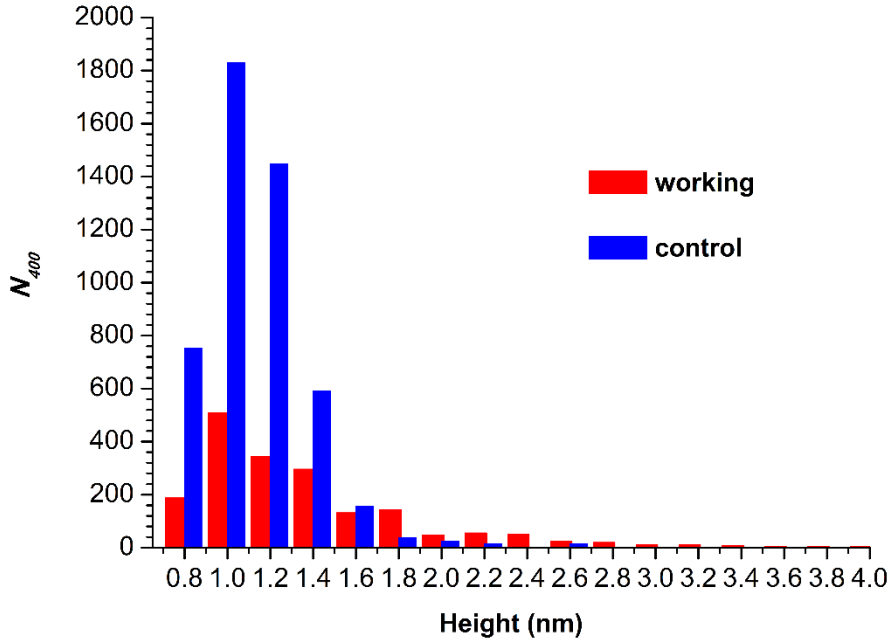

Figure 4. Histograms of N_{400} plotted vs. height for control (black bars) and working (red bars) HRP samples.

The N_{400} obtained for the working sample was $N_{400}(working)$ = 1876 particles/400 μm². For the control sample, the N_{400} value was higher (though of the same order of magnitude), amounting to 4867 particles/400 μm².

As regards the spectrophotometry results, no difference in the activity of the enzyme against ABTS between the working and the control sample was observed.

4. Discussion

In the Introduction, we have mentioned the long-term effect, which was observed after the incubation of the HRP enzyme near the inlet and the outlet linear sections of the heat exchanger with stopped flow of glycerol [19]. In the previously studied case, both the adsorption properties and the enzymatic activity of HRP were found to be affected. Now, we present the results of our recent experiments performed in the continuation of our studies in this respect. In the experiments reported herein, we have found that the incubation of HRP in the vicinity of the outer side of the cylindrical coiled heat exchanger with stopped glycerol flow also leads to a long-term effect on the enzyme aggregation state. At the same time, no effect on the enzymatic activity of HRP against its substrate ABTS has been revealed. The latter circumstance is in contrast to the situation observed previously [19], when the incubation of HRP sample near the inlet section of the heat exchanger markedly influenced the HRP-catalyzed kinetics of ABTS oxidation.

As regards the AFM study of the aggregation of the enzyme, its incubation in the vicinity of the heat exchanger with stopped glycerol flow has been found to cause an increase in the degree of HRP aggregation in comparison with the control enzyme sample. Such an increase observed in working experiments can be explained by a change in the hydration shell of the enzyme globule. This change can well occur in the course of the 40-min-long incubation of the enzyme sample near the heat exchanger with stopped glycerol flow [19]. The change in the hydration shell of HRP enzyme molecules can influence their interactions with each other [46] as well as with the mica substrate surface [47,48]. This effect could be associated with long-lived perturbations resulting from formation of nanobubble clusters [49]. Bunkin et al. [49] observed this phenomenon using a fluorescence-based technique, and explained it by an electromagnetic perturbation induced by an external

 doi:10.20944/preprints202403.0304.v1

electromagnetic field in aqueous solutions. In our work, electromagnetic radiation can occur at the expense of the triboelectric generation of charge, as was noted in the Introduction [16,17].

Of note, Beaufils et al. [47] have mentioned electromagnetic radiation within the list of factors influencing protein structure. Accordingly, adsorption and aggregation properties of the HRP glycoprotein can also be affected in this way. The long-term effect on the enzyme has been clearly observed (see Figure 3). This phenomenon can be explained by the influence of electromagnetic fields of non-trivial topology, which are known as "knotted" electromagnetic fields [20].

5. Conclusions

By AFM, we have revealed a long-term effect of electromagnetic field, generated triboelectrically by the flow of glycerol, on the adsorption properties of HRP enzyme. Namely, increased content of aggregated form of HRP has been observed on mica after a 40-min incubation of 0.1 μM buffered solution of the enzyme at a 2 cm distance from the coil with stopped flow of glycerol. We explain this phenomenon by the influence of electromagnetic fields of non-trivial topology on the enzyme's hydration shell. Enzymatic activity of HRP against its substrate ABTS remained unchanged, indicating no influence on the conformation of the enzyme's active site. This is an important point, since water is also known to be incorporated into active sites of enzymes [50]. Accordingly, in our experiments, only outer hydration shells have been affected. Considering the ubiquitous presence of electromagnetic fields in both the industry and the everyday life, we believe that the results of our study reported herein will help the researchers to better understand the role of these external factors in the functioning of enzyme systems.

Author Contributions: Conceptualization, Yuri D. Ivanov and Vadim Yu. Tatur; Data curation, Anastasia A. Valueva, Maria O. Ershova, Ivan D. Shumov, and Andrey F. Kozlov; Formal analysis, Ivan D. Shumov, Nina D. Ivanova, and Alexander N. Ableev; Investigation, Yuri D. Ivanov, Ivan D. Shumov, Anastasia A. Valueva, Irina A. Ivanova, Maria O. Ershova, and Vadim S. Ziborov; Methodology, Yuri D. Ivanov and Vadim Yu. Tatur; Project administration, Yuri D. Ivanov; Resources, Vadim Yu. Tatur, Andrei A. Lukyanitsa and Vadim S. Ziborov; Software, Andrei A. Lukyanitsa; Supervision, Yuri D. Ivanov; Validation, Vadim S. Ziborov; Visualization, Ivan D. Shumov, Andrey F. Kozlov and Anastasia A. Valueva; Writing – original draft, Ivan D. Shumov and Yuri D. Ivanov; Writing – review & editing, Yuri D. Ivanov.

Funding: This work was performed within the framework of the Program for Basic Research in the Russian Federation for a long-term period (No. 122030100168-2).

Data Availability Statement: Correspondence and requests for materials should be addressed to Y.D.I.

Acknowledgments: The AFM measurements were performed employing a Titanium multimode atomic force microscope, which pertains to "Avogadro" large-scale research facilities.

Conflicts of Interest: The authors declare no conflict of interest.

References

1. Robinson, P.K. Enzymes: principles and biotechnological applications. *Essays Biochem*. **2015**, *59*, 1-41. doi: 10.1042/BSE0590001.
2. Hu, S.; Lu, Q.; Xu, Y. Biosensors based on direct electron transfer of protein. In *Electrochemical Sensors, Biosensors and their Biomedical Applications*. X. Zhang, H. Ju, J. Wang, Eds. Academic Press, 2008. pp.531-581. DOI:10.1016/B978-012373738-0.50019-2.
3. Metzler, D.E. Biochemistry, the Chemical Reactions of Living Cells, 1st ed.; Academic Press: Cambridge, UK, 1977.
4. https://infinitabiotech.com/blog/top-5-applications-of-enzymes-in-biotechnology/
5. Buket, C.A.; Ay¸se, A.; Selçuk, K.; Süleyman, O.; Emel, S.Ç. Comparison of HCV core antigen and anti-HCV with HCV RNA results. *Afr. Health Sci*. **2014**, *14*, 816–820. DOI: 10.4314/ahs.v14i4.7.
6. Köroğlu, M.; Ak, S.; Ak, M.; Yakupoğulları, Y.; Özer, A. Evaluation of diagnostic performance of new antigen-based enzyme immune assay for diagnosis of Hepatitis C virus (HCV) infections. *Afr. J. Microbiol. Res.* **2012**, *6 (4)*, 809-812. DOI: 10.5897/AJMR11.1130.
7. Rigoldi, F.; Donini, S.; Giacomina, F.; Sorana, F.; Redaelli, A.; Bandiera, T.; Parisini, E.; Gautieri, A. Thermal stabilization of the deglycating enzyme Amadoriase I by rational design. *Sci. Rep*. **2018**, *8*, 3042. https://doi.org/10.1038/s41598-018-19991-x.

8. Mesbah, N.M. Industrial Biotechnology Based on Enzymes From Extreme Environments. *Front. Bioeng. Biotechnol*. **2022**, *10*, 870083. doi: 10.3389/fbioe.2022.870083.
9. Xiong, J.; Sun, Z.; Yu, J.; Liu, H.; Wang, X. Thermal self-regulatory smart biosensor based on horseradish peroxidase-immobilized phase-change microcapsules for enhancing detection of hazardous substances. *Chem. Eng. J.* **2022**, *430 (3)*, 132982. https://doi.org/10.1016/j.cej.2021.132982.
10. Sun, Z.; Liu, H.; Wang, X. Thermal self-regulatory intelligent biosensor based on carbon-nanotubes-decorated phase-change microcapsules for enhancement of glucose detection. *Biosens. Bioelectron.* **2022**, *195*, 113586. https://doi.org/10.1016/j.bios.2021.113586.
11. Doran, P.M. Heat transfer. In: Bioprocess Engineering Principles, 2nd ed.; Doran, P.M. Ed.; Academic Press. Elsevier Ltd.: Oxford, UK, 2013 pp. 333-377. DOI: 10.1016/B978-0-12-220851-5.00009-5.
12. Fakhrulrezza, M.; Ahn, J.; Lee, H.-J. Thermal Design of a Biohydrogen Production System Driven by Integrated Gasification Combined Cycle Waste Heat Using Dynamic Simulation. *Energies* **2022**, *15*, 2976. https://doi.org/10.3390/en15092976.
13. Kushchev, L.A.; Okuneva, G.L.; Suslov, D.Y.; Gravin, A.A. Modeling biogas production in bubbling bioreactors. *Chem. Petrol. Eng*. **2012**, *47*, 613–618. https://doi.org/10.1007/s10556-012-9519-1.
14. Zhang, T.; Liu, C.; Gu, Y.; Jérôme, F. Glycerol in Energy Transportation: A State-of-the-art Review. *Green Chem.* **2021**, 7865-7889. OI: https://doi.org/10.1039/D1GC02597J.
15. Widya, P.S.; Asep, B.D.N. Design of Glycerol-Water-Based Heat Exchanger for The Production of Silicon Dioxide (SiO_2) Nanoparticles. *Maghr. J. Pure Appl. Sci.* **2022**, 8 (1), 41-50. https://doi.org/10.48383/IMIST.PRSM/mjpas-v8i1.36091.
16. Yoo, D.; Jang, S.; Cho, S.; Choi, D.; Kim, D.S. A Liquid Triboelectric Series. *Adv. Mater*. **2023**, 2300699. DOI: 10.1002/adma.202300699.
17. Tanasescu, F.; Cramariuc, R. Electroststica în Technica; Editura Technica: Bucuresti, Romania, 1977.
18. Ivanov, Y.D.; Shumov, I.D.; Kozlov, A.F.; Ershova, M.O.; Valueva, A.A.; Ivanova, I.A.; Tatur, V.Y.; Lukyanitsa, A.A.; Ivanova, N.D.; Ziborov, V.S. Glycerol Flow through a Shielded Coil Induces Aggregation and Activity Enhancement of Horseradish Peroxidase. *Appl. Sci*. **2023**, *13*, 7516. https://doi.org/10.3390/app13137516.
19. Ivanov, Y.D.; Shumov, I.D.; Kozlov, A.F.; Ershova, M.O.; Valueva, A.A.; Ivanova, I.A.; Tatur, V.Y.; Lukyanitsa, A.A.; Ivanova, N.D.; Ziborov, V.S. Stopped Flow of Glycerol Induces the Enhancement of Adsorption and Aggregation of HRP on Mica. *Micromachines* **2023**, *14*, 1024. https://doi.org/10.3390/mi14051024.
20. Ivanov, Y.D.; Pleshakova, T.O.; Shumov, I.D.; Kozlov, A.F.; Ivanova, I.A.; Valueva, A.A.; Tatur, V.Y.; Smelov, M.V.; Ivanova, N.D.; Ziborov, V.S. AFM imaging of protein aggregation in studying the impact of knotted electromagnetic field on a peroxidase. *Sci. Rep.* **2020**, *10*, 9022. https://doi.org/10.1038/s41598-020-65888-z.
21. Housmans, J.A.J.; Wu, G.; Schymkowitz, J.; Rousseau, F. A guide to studying protein aggregation. *FEBS J.* **2023**, *290*, 554–583. https://doi.org/10.1111/febs.16312
22. Louros, N., Schymkowitz, J. & Rousseau, F. Mechanisms and pathology of protein misfolding and aggregation. *Nat. Rev. Mol. Cell. Biol.* **2023**, *24*, 912–933. https://doi.org/10.1038/s41580-023-00647-2.
23. Colombo, G.; Meli, M.; De Simone, A. Computational studies of the structure, dynamics and native content of amyloid-like fibrils of ribonuclease A. *Proteins* **2008**, *70*, 863–872. DOI: 10.1002/prot.21648.
24. Laage, D.; Elsaesser, T.; Hynes, J.T. Water Dynamics in the Hydration Shells of Biomolecules. *Chem. Rev*. **2017**, *117*, 10694−10725. https://doi.org/10.1021/acs.chemrev.6b00765.
25. Chakraborty, I.; Kar, R.K.; Sarkar, D.; Kumar, S.; Maiti, N.C.; Mandal, A.K.; Bhunia, A. Solvent Relaxation NMR: A Tool for Real-Time Monitoring Water Dynamics in Protein Aggregation Landscape. *ACS Chem. Neurosci.* **2021**, *12*, 2903-2916. https://doi.org/10.1021/acschemneuro.1c00262.
26. Schramm, F.D.; Schroeder, K.; Jonas, K. Protein aggregation in bacteria. *FEMS Microbiol. Rev*. **2020**, *44(1)*, 54–72. https:// doi. org/ 10.1093/ femsre/ fuz026.
27. Colombie, S.; Gaunand, A.; Lindet, B. Lysozyme inactivation and aggregation in stirred-reactor. *J. Mol. Catalysis* B: *Enzymatic* **2001**, *11*, 559-565. https://doi.org/10.1016/S1381-1177(00)00044-8.
28. Gentile, K.; Bhide, A.; Kauffman, J.; Ghosh, S.; Maiti, S.; Adair, J.; Lee, T.-H.; Sen, A. Enzyme aggregation and fragmentation induced by catalysis relevant species. *Phys. Chem. Chem. Phys*. **2021**, 23, 20709–20717. https://doi.org/10.1039/D1CP02966E.
29. Sun, J.; Sun, F.; Xu, B.; Gu, N. The quasi-one-dimensional assembly of horseradish peroxidase molecules in presence of the alternating magnetic field. *Coll. Surf. A: Physicochem. Eng. Aspects* **2010**, *360 (1-3)*, 94-98. https://doi.org/10.1016/j.colsurfa.2010.02.012.
30. Sun, J; Zhou, H.; Jin, Y.; Wang, M.; Gu, N. Magnetically enhanced dielectrophoretic assembly of horseradish peroxidase molecules: chaining and molecular monolayers. *Chem. Phys. Chem.* **2008**, *9(13)*, 1847-1850. https://doi.org/10.1002/cphc.200800237.
31. Ivanov, Y.D.; Tatur, V.Y.; Pleshakova, T.O.; Shumov, I.D.; Kozlov, A.F.; Valueva, A.A.; Ivanova, I.A.; Ershova, M.O.; Ivanova, N.D.; Repnikov, V.V.; et al. Effect of Spherical Elements of Biosensors and

Bioreactors on the Physicochemical Properties of a Peroxidase Protein. *Polymers* **2021**, *13*, 1601. https://doi.org/10.3390/polym13101601.

32. Davies, P. F., Rennke, H. G. & Cotran, R. S. Influence of molecular charge upon the endocytosis and intracellular fate of peroxidase activity in cultured arterial endothelium. *J. Cell Sci.* **1981,** *49*(1), 69–86. 86. https://doi.org/10.1242/jcs.49.1.69.
33. Welinder, K.G. Amino acid sequence studies of horseradish peroxidase. amino and carboxyl termini, cyanogen bromide and tryptic fragments, the complete sequence, and some structural characteristics of horseradish peroxidase C. *Eur. J. Biochem*. **1979**, *96*, 483–502. https://doi.org/10.1111/j.1432-1033.1979.tb13061.x.
34. Matsui, T.; Hori, M.; Shizawa, N.; Nakayama, H.; Shinmyo, A.; Yoshida, K. High-efficiency secretory production of peroxidase C1a using vesicular transport engineering in transgenic tobacco. *J. Biosci. Bioeng*. **2006**, *102 (2)*, 102-109. https://doi.org/10.1263/jbb.102.102.
35. Krainer, F.W.; Glieder, A. An updated view on horseradish peroxidases: Recombinant production and biotechnological applications. *Appl. Microbiol. Biotechnol*. **2015**, *99*, 1611–1625. https://doi.org/10.1007/s00253-014-6346-7.
36. Yao, Y.; Zhang, B.; Pang, H.; Wang, Y.; Fu, H.; Chen, X.; Wang, Y. The effect of radio frequency heating on the inactivation and structure of horseradish peroxidase. *Food Chem*. **2023**, *398*, 133875. https://doi.org/10.1016/j.foodchem.2022.133875.
37. Bayramoglu, G.; Arıca, M.Y. Enzymatic removal of phenol and p-chlorophenol in enzyme reactor: Horseradish peroxidase immobilized on magnetic beads. *J. Hazard. Mater*. **2008**, *156*, 148–155. https://doi.org/10.1016/j.jhazmat.2007.12.008.
38. Ramanavicius, A.; Kausaite-Minkstimiene, A.; Morkvenaite-Vilkonciene, I.; Genys, P.; Mikhailova, R.; Semashko, T.; Voronovic, J.; Ramanaviciene, A. Biofuel cell based on glucose oxidase from Penicillium funiculosum 46.1 and horseradish peroxidase. *Chem. Eng. J.* **2015**, *264*, 165-173. https://doi.org/10.1016/j.cej.2014.11.011.
39. Chung, Y.; Tannia, D.C.; Kwon, Y. Glucose biofuel cells using bi-enzyme catalysts including glucose oxidase, horseradish peroxidase and terephthalaldehyde crosslinker. *Chem. Eng. J.* **2018**, *334*, 1085-1092. https://doi.org/10.1016/j.cej.2017.10.121.
40. Abreau, C.; Nedellec, Y.; Ondel, O.; Buret, F.; Cosnier, S.; Le Goff, A.; Holzinger, M. Glucose oxidase bioanodes for glucose conversion and H_2O_2 production for horseradish peroxidase biocathodes in a flow through glucose biofuel cell design. *J. Power Sources* **2018**, *392*, 176-180. https://doi.org/10.1016/j.jpowsour.2018.04.104.
41. Warille, A.A.; Altun, G.; Elamin, A.A.; Kaplan, A.A.; Mohamed, H.; Yurt, K.K.; Elhaj, A.E. Skeptical approaches concerning the effect of exposure to electromagnetic fields on brain hormones and enzyme activities. *J. Microsc. Ultrastruct.* **2017**, *5*, 177–184. http://dx.doi.org/10.1016/j.jmau.2017.09.002.
42. Kiselyova, O.I.; Yaminsky, I.; Ivanov, Y.D.; Kanaeva, I.P.; Kuznetsov, V.Y.; Archakov, A.I. AFM study of membrane proteins, cytochrome P450 2B4, and NADPH–Cytochrome P450 reductase and their complex formation. *Arch. Biochem. Biophys.* **1999**, *371*, 1–7. https://doi.org/10.1006/abbi.1999.1412.
43. Pleshakova, T.O.; Kaysheva, A.L.; Shumov, I.D.; Ziborov, V.S.; Bayzyanova, J.M.; Konev, V.A.; Uchaikin, V.F.; Archakov, A.I.; Ivanov, Y.D. Detection of hepatitis C virus core protein in serum using aptamer-functionalized AFM chips. *Micromachines* **2019**, *10*, 129. https://doi.org/10.3390/mi10020129.
44. Sanders, S.A.; Bray, R.C.; Smith, A.T. pH-dependent properties of a mutant horseradish peroxidase isoenzyme C in which Arg38 has been replaced with lysine. *Eur. J. Biochem.* **1994**, *224*, 1029–1037. https://doi.org/10.1111/j.1432-1033.1994.01029.x.
45. Drozd, M.; Pietrzak, M.; Parzuchowski, P.G.; Malinowska, E. Pitfalls and capabilities of various hydrogen donors in evaluation of peroxidase-like activity of gold nanoparticles. *Anal. Bioanal. Chem.* **2016**, *408*, 8505–8513. https://doi.org/10.1007/s00216-016-9976-z.
46. Vitagliano, L.; Berisio, R.; De Simone, A. Role of Hydration in Collagen Recognition by Bacterial Adhesins. *Biophys. J.* **2011**, *100*, 2253-2261. doi: 10.1016/j.bpj.2011.03.033.
47. Beaufils, C.; Man, H.-M.; de Poulpiquet, A.; Mazurenko, I.; Lojou, E. From Enzyme Stability to Enzymatic Bioelectrode Stabilization Processes. *Catalysts* **2021**, *11*, 497. https://doi.org/10.3390/catal11040497.
48. Ziborov, V.S.; Pleshakova, T.O.; Shumov, I.D.; Kozlov, A.F.; Valueva, A.A.; Ivanova, I.A.; Ershova, M.O.; Larionov, D.I.; Evdokimov, A.N.; Tatur, V.Y.; et al. The Impact of Fast-Rise-Time Electromagnetic Field and Pressure on the Aggregation of Peroxidase upon Its Adsorption onto Mica. *Appl. Sci.* **2021**, *11*, 11677. https://doi.org/10.3390/app112411677.
49. Bunkin, N.F.; Bolotskova, P.N.; Bondarchuk, E.V.; Gryaznov, V.G.; Gudkov, S.V.; Kozlov, V.A.; Okuneva, M.A.; Ovchinnikov, O.V.; Smoliy, O.P.; Turkanov, I.F. Long-Term Effect of Low-Frequency Electromagnetic Irradiation in Water and Isotonic Aqueous Solutions as Studied by Photoluminescence from Polymer Membrane. *Polymers* **2021**, *13*, 1443. https://doi.org/10.3390/polym13091443.
50. Fusco, G.; Biancaniello, C.; Vrettas, M.D.; De Simone, A. Thermal tuning of protein hydration in a hyperthermophilic enzyme. *Front. Mol. Biosci*. **2022**, *9*, 1037445. doi: 10.3389/fmolb.2022.1037445.

 doi:10.20944/preprints202403.0304.v1